2018 IEEE International Conference on Robotics and Automation (ICRA)
May 21-25, 2018, Brisbane, Australia

Autonomous Multi-Joint Soft Exosuit for Assistance with Walking Overground

Sangjun Lee, *Student Member, IEEE*, Nikos Karavas, Brendan T. Quinlivan, Danielle Louise Ryan, David Perry, Asa Eckert-Erdheim, Patrick Murphy, Taylor Greenberg Goldy, Nicolas Menard, Maria Athanassiu, Jinsoo Kim, Giuk Lee, Ignacio Galiana, and Conor J. Walsh, *Member, IEEE*

Abstract— **Soft exosuits are a new approach for assisting with human locomotion, which applies assistive torques to the wearer through functional apparel. In this paper, we present a new version of autonomous multi-joint soft exosuit for gait assistance, particularly designed for overground walking. The soft exosuit assists with ankle plantarflexion, hip flexion, and hip extension, equally distributing the forces between ankle plantarflexion and hip flexion. A mobile actuation system was developed to generate high assistive forces, and Bowden cables are used to transmit the forces to the exosuit. A sensor harness connects two load cells and three IMUs per leg that are used to measure real-time data for a controller that commands desired force profiles as a function of the walking cycle. In addition, a control adaptation method was developed which adjusts control parameters while walking on irregular surfaces. In preliminary studies, the proposed method substantially improved the force consistency while walking over uneven terrain. Specifically, the number of steps where the peak force deviated from the target force decreased from 100 to 57 out of 250 steps, and RMS error on the peak force decreased from 90.0 N to 76.6 N with respect to 300 N target force. Also, a two-subject case study on country-course walking demonstrated the potential of this soft exosuit to improve human energy economy while walking overground.**

I. Introduction

Over the past decade, lower-limb wearable devices have been developed to assist with human walking. Applications of these devices include assisting individuals with disabilities to relieve their gait deficits [1-2] and augmenting healthy people to improve the energy economy during walking [3-5] or load carriage [6-7]. Conventionally these devices have consisted of rigid structures which enables to deliver high assistive torques to the wearer and to transfer carried load directly to the ground [7]. However, when misaligned with the wearer's biological joints, the rigid frames may restrict the natural motion of the wearer and apply undesired forces [7-8]. Moreover, rigid structures may add large inertia to the wearer's lower limb, which is associated with increased energy expenditure during walking [9].

This material is based upon the work supported by the Defense Advanced Research Projects Agency (DARPA), Warrior Web Program (Contract No. W911NF-14-C-0051), the Samsung Scholarship, and the NSF Graduate Research Fellowship Program (Grant No. DGE1144152). This work was also partially funded by the Wyss Institute for Biologically Inspired Engineering and the John A. Paulson School of Engineering and Applied Sciences at Harvard University.

S. Lee (slee@seas.harvard.edu), N. Karavas, B. T. Quinlivan, D. L. Ryan, D. Perry, A. Eckert-Erdheim, P. Murphy, T. Greenberg Goldy, N. Menard, M. Athanassiu, J. Kim, G. Lee, I. Galiana, and C. J. Walsh (617-496-7128; walsh@seas.harvard.edu) are with the John A. Paulson School of Engineering and Applied Sciences and the Wyss Institute for Biologically Inspired Engineering, Harvard University, MA 02138, USA.

To address some of these challenges, several groups have recently used low-profile components to anchor to the body and apply assistive torques to a single joint in parallel with the underlying muscles [3-6, 10-11]. Recent lab-based studies have shown that such devices may substantially reduce the metabolic cost of walking. While many of these systems were tethered and only reported gross metabolic reductions relative to walking with the device unpowered [3, 10], some studies have found net metabolic reductions relative to walking without wearing the device. Lee *et al.* reported a 21.1% net reduction relative to walking without wearing the device for unloaded walking, using an autonomous hip exoskeleton assisting with both flexion and extension [11]. For ankle exoskeletons, Mooney *et al.* reported an 8% net reduction for loaded walking [6] and a 11% net reduction for unloaded walking [5], compared to a no-device condition.

Following the trend of wearable devices targeting specific joint motions with lightweight components, our group has been using functional apparel to comfortably anchor to the body and deliver assistance to specific target joints, creating "soft exosuits" [12-20]. In recent studies, soft exosuits assisting with hip, ankle, or both joints have significantly reduced the energy cost of walking [14-15], load carriage [16-17], and even running [18]. Among them was Panizzolo *et al.* (2016) which demonstrated that an autonomous multi-joint soft exosuit assisting with ankle plantarflexion, hip flexion, and hip extension [13] significantly reduced the net metabolic cost of loaded walking by 7.3%, compared to equivalent-mass-removed condition (EMR; walking with the device unpowered but removing the equivalent mass of the device) [16]. While it showed great promise as the first successful study to reduce the metabolic burden of load carriage with a fully mobile multi-joint assistive device, there still remained much scope to improve its performance given a number of limitations to this prototype and the study.

Therefore, in this paper, we present a new version of autonomous multi-joint soft exosuit (Fig. 1A) by improving each aspect of the system, i.e. suit, actuation, and control, as well as the study design, based on the lessons learned from [16] as follows:

1) *Suit:* Though the multi-articular nature of the suit textile architecture successfully created both ankle plantarflexion and hip flexion assistance using a single actuator in [16], the force distribution between the two joints was not consistent across different users and trials and even on a step-by-step basis, particularly when walking overground. This was because the force distribution was highly dependent on the adjustment of the multi-articular straps, which was sensitive to the suit donning procedure as well

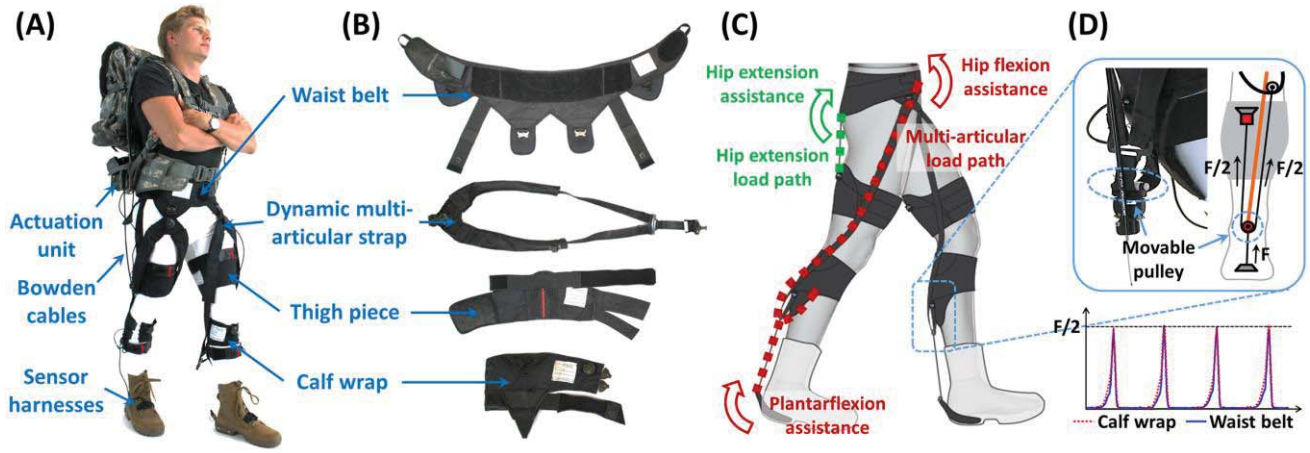

Figure 1 **(A)** The autonomous multi-joint soft exosuit for gait assistance. Textile components (waist belt, dynamic multi-articular strap, thigh piece, and calf wrap) are discussed in Section II, and hardware components (actuation unit, Bowden cable, and sensor harness) are discussed in Section III. **(B)** Textile components of the exosuit: a waist belt, a dynamic multi-articular strap (left), a thigh piece (left), and a calf wrap (left). **(C)** Load paths created by the textile architecture. The hip extension load path (green dotted line) creates hip extension assistance (green arrow), while the multi-articular load path (red dotted line) creates ankle plantarflexion and hip flexion assistance (red arrows). **(D)** A close-up photo and a schematic diagram of the movable pulley mechanism of the dynamic multi-articular strap, which evenly distributes the assistive forces between the calf wrap and the waist belt. The graph on the bottom shows representative data from a preliminary evaluation testing; the forces measured at the calf wrap and the waist belt over four consecutive strides were almost identical, demonstrating the force distribution performance of the dynamic multi-articular strap.

as the step-to-step variability in the wearer's lower-limb kinematics. In the updated version of the exosuit presented here, we have developed apparel components that are more lightweight and capable of equally distributing assistive forces between ankle plantarflexion and hip flexion through dynamic multi-articular straps.

2) *Actuation:* While a significant amount of metabolic benefit was shown in [16], the peak assistive forces were limited to 272 N for ankle plantarflexion, 204 N for hip flexion, and 68 N for hip extension (Equivalent peak assistive moments were 24.8 Nm, 21.8 Nm, and 9.9 Nm, respectively) due to the actuator capability. As suggested by Quinlivan *et al.* for ankle [14] and by Ding *et al.* for hip [17], when an exosuit delivers higher assistive forces, it may provide increased metabolic benefit to the user. Therefore, in this paper, we present a new actuation system which is capable of generating higher assistive forces with a more compact form factor enabling it to be mounted closer to the body center of mass.

3) *Control:* In [16], the assistance profiles were designed simply by down-scaling the biological joint moment patterns. More recently, however, by using offboard actuation systems, we explored different control strategies for both hip extension assistance [19] and multi-articular (ankle plantarflexion and hip flexion) assistance [20], and found control parameters which may result in a higher metabolic benefit. In this version, we have implemented these control strategies by improving sensing and computation capability of the device.

4) *Adaptation to uneven terrain:* To be a successful mobile assistive device for real-world environment, the controller must work robustly over different walking terrains. In previous versions, the high-level controllers were designed based only on biological joint moment and power patterns of flat-ground walking [16]; however, on uneven terrains, kinetics and kinematics greatly differ compared to those of walking on a treadmill or a flat ground [21]. In this paper, we propose a control adaptation method which adjusts multi-articular assistance profile depending on foot contact conditions on mild uneven terrains, inspired by human's natural kinetic/kinematic adaptation when stepping on a small bump while walking [21].

5) *Study design:* While the device was fully mobile and untethered in [16], the evaluation study was still confined to a lab-based experiment on a treadmill. Also, since the EMR condition was used for the baseline comparison, instead of a no-device condition, the true benefit of using the device was not clearly demonstrated. In this paper, we conducted a preliminary human subject study where we evaluated the metabolic cost of load carriage over an outdoor country course, relative to walking without the device.

II. Soft Exosuit

The soft exosuit used in this study is shown in Figure 1A, which improves upon the multi-joint exosuit that have been reported by our group [13]. The suit was designed to assist with ankle plantarflexion, hip flexion, and hip extension, which together generate more than 2/3 of the total lower-limb joint work while walking on flat or irregular surfaces [21].

The suit consists of a spandex base layer and a waist belt, and a thigh piece, a calf wrap, and a dynamic multi-articular strap on each leg (Fig. 1B). The base layer includes high-friction Fabrifoam (Fabrifoam Products, Exton, PA, USA) insets to securely anchor to the wearer's skin and minimize drift or migration of the suit components. The waist belt anchors to the wearer's pelvis which can bear relatively high forces compared to other parts of the body. It is secured with Velcro at center front, accommodating different body types. The thigh piece wraps around the user's thigh and closes with Velcro tabs, conforming around various thigh shapes. The calf wrap anchors above the convex geometry of the wearer's calf muscles. It closes with a Boa System (Boa Technology Inc., Denver, CO, USA), which facilitates donning and doffing and adjusts its compression level. The dynamic

multi-articular strap connects the calf wrap to the waist belt and distributes the actuation load between the calf and the waist, similarly to [20]. One end of the strap is attached to a buckle in front of the waist belt at the top of the leg, while the other end is attached to a buckle at the back of the calf wrap. The strap was designed to pass through the medial and lateral sides of the knee joint. These apparel components were manufactured in different sizes from XS to XXL. For a medium size, the waist belt, the thigh piece, the calf wrap, and the dynamic multi-articular strap weigh 240 g, 97 g (per leg), 93 g (per leg), and 138 g (per leg), respectively, which make 896 g in total. Finally, a metal bracket (50 g) is bolted to the back of each military boot, and a textile boot cover (52 g) wraps around the wearer's ankle on each side.

Load paths configured by the textile architecture are similar to the ones previously presented in [13]: a hip extension load path and a multi-articular load path (Fig. 1C). In general, the load paths create assistive forces on the body in parallel with the wearer's underlying muscles; if the forces are applied at the right timing, activations of those muscles as well as the energy cost of walking may decrease due to the human adaptation of locomotion to external assistance [10, 15]. The hip extension load path assists with hip extension during early stance, aiming to unburden hip extensor muscles (e.g. biceps femoris, gluteus maximus). The multi-articular load path simultaneously assists with ankle plantarflexion and hip flexion during the mid and late stance phases, assisting ankle plantarflexor (e.g. gastrocnemius, soleus) and hip flexor muscles (e.g. rectus femoris, psoas).

One of the key improvements in this version of the exosuit is the dynamic multi-articular strap, which distributes the multi-articular assistive forces evenly between the calf and the waist (Fig. 1D). Unlike previous versions where the multi-articular straps statically connect the calf wraps and the waist belt [13], the new straps are routed over movable pulleys which dynamically move along the straps and divide the forces equally in half. As shown in the bottom graph in Figure 1D, in a preliminary evaluation testing, the dynamic multi-articular strap demonstrated the capability to evenly distribute the forces while walking.

III. Hardware Implementation

A. Actuation System

Figure 2 shows mechanical design and implementation of the mobile actuation system; overall, two hip extension actuator units and two multi-articular actuator units are joined to form a single compact actuation system which can be bolted to the lower back frame of a military rucksack close to the wearer's body center of mass. The actuator units were designed and built in-house with Emoteq frameless 6-pole motors (QB01701 for hip extension, SQB02300 for multi-articular actuators; Allied Motion Inc., Amherst, NY, USA). Torques from the motors are transmitted through helicon gears (Spiroid Gearing; Illinois Tool Works, Inc., Glenview, IL, USA) at a gearing ratio of 36:1 for hip extension and 38:1 for the multi-articular actuators. Multi-wrap pulleys with covers are attached to the other end of the gears, which have 55-mm diameter for both hip extension and multi-articular actuators. The actuation system is capable of delivering peak forces up to 350 N through multi-articular load path and up to 250 N through hip extension load path (Equivalent peak

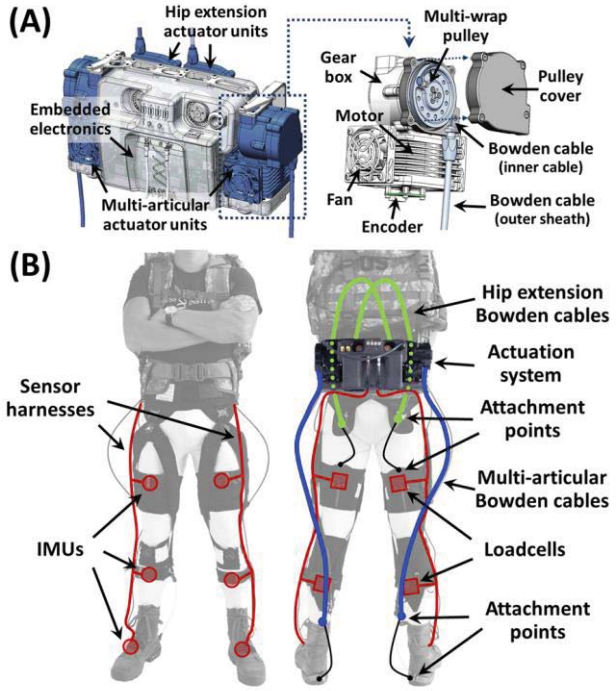

Figure 2 (A) A 3-D CAD model of the mobile actuation system, consisting of four actuator units (left and right, hip extension and multi-articular assistance). **(B)** Implementation of hardware components. The actuation system is mounted at the lower back frame of a military rucksack. Multi-articular Bowden cables (blue lines) route naturally down to the back of the calf on the same side. Hip extension Bowden cables (green lines) first travel up and turn back down to the back of the hip on the other side. Sensor harnesses (red lines), consisting of three IMUs (red circles) and two load cells (red rectangles) per leg, route down along the lateral side of the wearer's legs from the back of the actuation system to the foot IMUs.

moments are 35 Nm for ankle plantarflexion, 17.5 Nm for hip flexion, and 25 Nm hip extension), spending about 80 W of electrical power for one hip extension actuator unit and about 60 W for one multi-articular actuator unit. The system weighs 5.1 kg, and is powered by a 48V-6.6Ahr Li-Po battery (1.7 kg) stowed in the rucksack.

As with the previous versions [12-20], Bowden cables are used to transmit the forces from the actuation system to the exosuit. On the actuator side (Fig. 2A), the outer sheath attaches to the frame of the pulley cover and its inner cable connects to the pulley. On the human side (Fig. 2B), for the hip extension load path, the sheath attaches to the back of the waist belt and the inner cable extends to the back of the thigh piece. For the multi-articular load path, the sheath connects to the movable pulley of the multi-articular strap and the inner cable extends to the bracket at the back of the boot. When the motor rotates inward, the distance between two attachment points is shortened, generating forces not only on the cable but also along the entire length of the textile load path. Note that, whereas multi-articular Bowden cables route naturally down to the same side's attachment points, hip extension Bowden cables first travel up into a space between the ruck frame and the wearer's back and then turn back down to the attachment points on the other side (Fig. 2B); this cable routing provides a sufficient service loop for the Bowden cables not to interfere with the wearer's natural motion of hip joint. All Bowden cables weigh about 0.8 kg in total.

B. Sensors and Electronics

Inertial measurement units (IMUs) and load cells are used to obtain real-time data from the wearer and the exosuit. On each leg, three IMUs (MTi-3 AHRS; Xsens Technologies B.V., Enschede, Netherlands) are mounted at center front of the thigh piece, center front of the calf wrap, and dorsal side of the boot. These IMUs are used to obtain sagittal-plane angular displacement and angular velocity of thigh, shank, and foot, respectively. Also, two load cells (LSB200; Futek Advanced Sensor Technology Inc., Irvine, CA, USA) per leg are used to measure the force on each load path; one is mounted at the back of the thigh piece in series with the Bowden cable for measuring the force on the hip extension load path, while the other is mounted at the back of the calf wrap in series with the dynamic strap to measure the force on the multi-articular load path. Note that, the measurement from the load cell at the calf wrap has to be doubled to get the full force along the load path, under the assumption that the dynamic multi-articular strap evenly divides the cable force between the calf wrap and the waist belt. To minimize electrical wiring, all sensors on each leg are integrated into a sensor harness with a linear daisy-chain topology through CAN communication (Fig. 2B); the IMUs are mounted on small custom boards that linearly connect to each other, and each load cell connects to its proximal IMU's board. The sensor harness including all sensors weighs 168 g per leg.

The embedded electronics consists of two identical custom boards, one for the hip extension actuation and the other for the multi-articular actuation. Each board integrates two motor controllers (Gold Twitter; Elmo Motion Control Ltd., Petach-Tikva, Israel) which drive the two motors for left and right legs by running a position control loop cascaded with a velocity loop. One 32-bit ARM microprocessor per board (Cortex-M7; Atmel Corporation, San Jose, CA, USA) operates the two motor controllers; it runs an embedded software that reads in all sensor data from the sensor harnesses, computes high-level control algorithms, handles all system peripherals, and sends required position commands to the motor controllers through CAN-open communication.

IV. General Control Approach

A. Low-level Control

In general, the low-level control approach is similar to that of previous-version exosuits [19-20], where we have distinguished two different phases in the force generation mechanism: the *pretension phase* and the *active force phase*. In an exosuit system driven by Bowden cables, the assistive force is determined by the relative deflection between two apparel anchor attachment points across the target joint (a function of textile and tissue compliance). Thus, the assistive force can be generated either passively by the kinematics of the joint while the motor is just holding the cable in a fixed position (pretension), or actively by retracting the cable by the motor (active force). As shown in Figure 3, in this approach, the active force is used as a primary means to deliver assistance during a target period within a gait cycle, e.g. the positive power phase at ankle [20], and the pretension is primarily used to keep the cable consistently tensioned as well as have an initial force level before applying the active assistance.

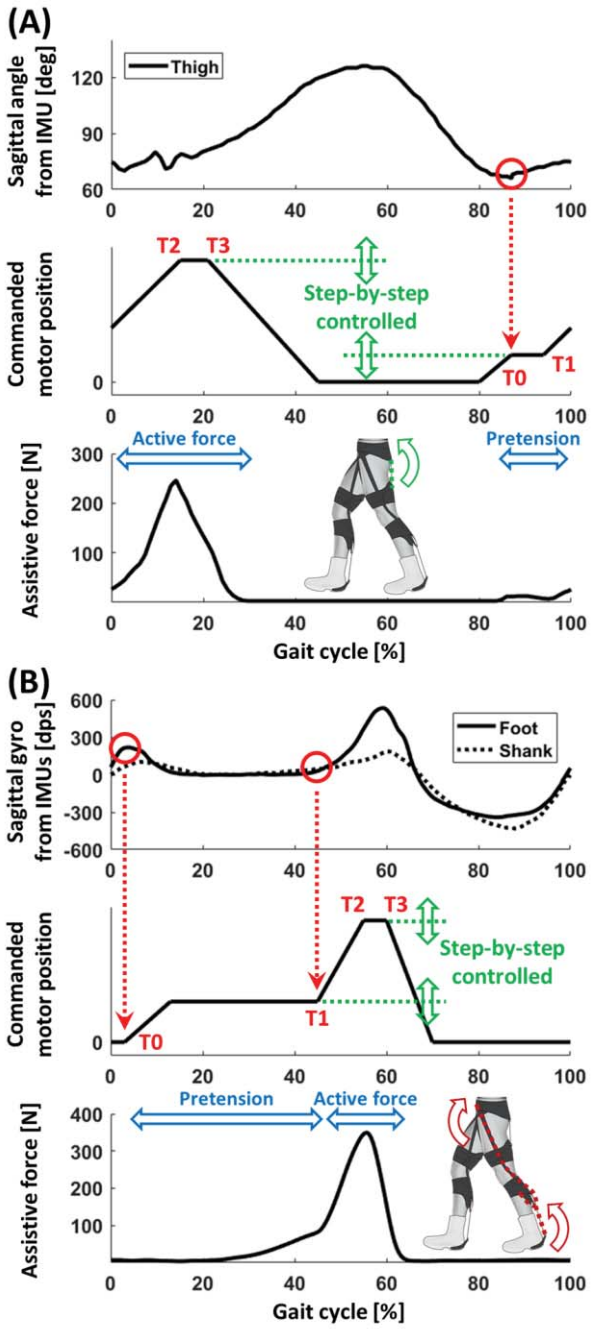

Figure 3 High-level control overview of the autonomous multi-joint soft exosuit. ***T0***, ***T1***, ***T2***, and ***T3*** are timing parameters defined in the position controller, indicating the start of pretension phase, the start of active force phase, the completion of cable pulling, and the end of active force phase, respectively. **(A)** Representative data illustrating hip extension assistance controller. It starts from the maximum hip flexion and applies assistance while hip extensor muscles are active. **(B)** Representative data illustrating multi-articular assistance controller. It starts from the heel strike and delivers the majority of assistance during the positive power phase at ankle.

To achieve a desired level of pretension and active force, the controller performs a force-based position control of the Bowden cables on a step-by-step basis, as described for previous system embodiments [19-20]. During each stride, the controller measures peak pretension and active force by monitoring the load cell data from the sensor harnesses. At the end of each stride, the controller makes decisions on the

cable position for the next stride, by comparing the desired and the measured peak pretension and active force. For example, if the measured peak active force is less than the desired, the controller decides to increase the cable retraction amplitude for the next stride; on the other hand, if the measured pretension is higher than the desired, the controller will decrease the cable holding position for the next stride. Note that the increment/decrement in cable position was pre-determined to be small enough, so that the controller aims not to achieve the desired force in the next stride right away but to gradually approach to the desired value over multiple strides. This strategy is similar in principle with the learning-based controller or once-per-step controller used in other assistive devices.

B. *High-level Control*

Given that the low-level controller regulates the cable position by separating the pretension phase and the active force phase, the high-level controller defines when each phase starts and ends within a gait cycle for the hip extension assistance and the multi-articular assistance, by using the sensor data available (Fig. 3).

Hip extension assistance. The high-level controller for the hip extension load path has been designed to apply assistive torques while hip extensor muscles are active, based on the assumption that this may reduce the activation of those muscles and consequently reduce the metabolic cost of walking, which is in principle similar to Ding *et al.* (2016) [19]. Since it has been reported that the hip extensor muscles are active starting from the maximum hip flexion while walking, the controller estimates the maximum hip flexion using the thigh IMU data and considers this as the key event to define the gait cycle as well as the average stride time (AST) over the last three strides. Starting from the maximum hip flexion, the controller generates a position trajectory that demonstrates similar onset, offset, and peak force timings to the ones of the biological hip joint moment. To be specific, as shown in Figure 3A, the controller regards the maximum hip flexion as the start of the pretension phase (***T0***) and keeps the cable position for 7% of AST until the start of the active force phase (***T1***). Then the motor retracts the cable for 21% of AST (until ***T2***) to generate active force and keeps the cable position for the next 6% of AST until the end of the active force phase (***T3***). Then, the motor releases the cable to avoid any interference during swing phase.

Multi-articular assistance. The high-level controller for the multi-articular load path has been designed to deliver the majority of assistance during the positive power phase at the ankle, which is in principle similar to Lee *et al.* (2016) (Fig 3B) [20]. While the wearer is walking with the exosuit, the controller first detects the heel strike using the sagittal-plane gyro signal from the foot IMU, and regards this as the start of the pretension phase (***T0***) (Note that the pretension force will be passively generated later in the gait cycle as the ankle dorsiflexes naturally). Then, the controller monitors the sagittal-plane gyro signals from the foot and the shank IMUs, to detect the zero-crossing of the ankle joint velocity which corresponds to the onset of the positive power phase at ankle [20]. This is considered as the start of the active force phase (***T1***), and the motor retracts the cable for 10% of the average stride time over the last three strides (until ***T2***) up to the cable retraction amplitude. The motor then keeps the cable in this position until the force at the shank load cell naturally drops, as the ankle joint further plantarflexes. This is determined as the end of active force phase (***T3***), and the motor spools the cable out to prevent resistance during the swing phase.

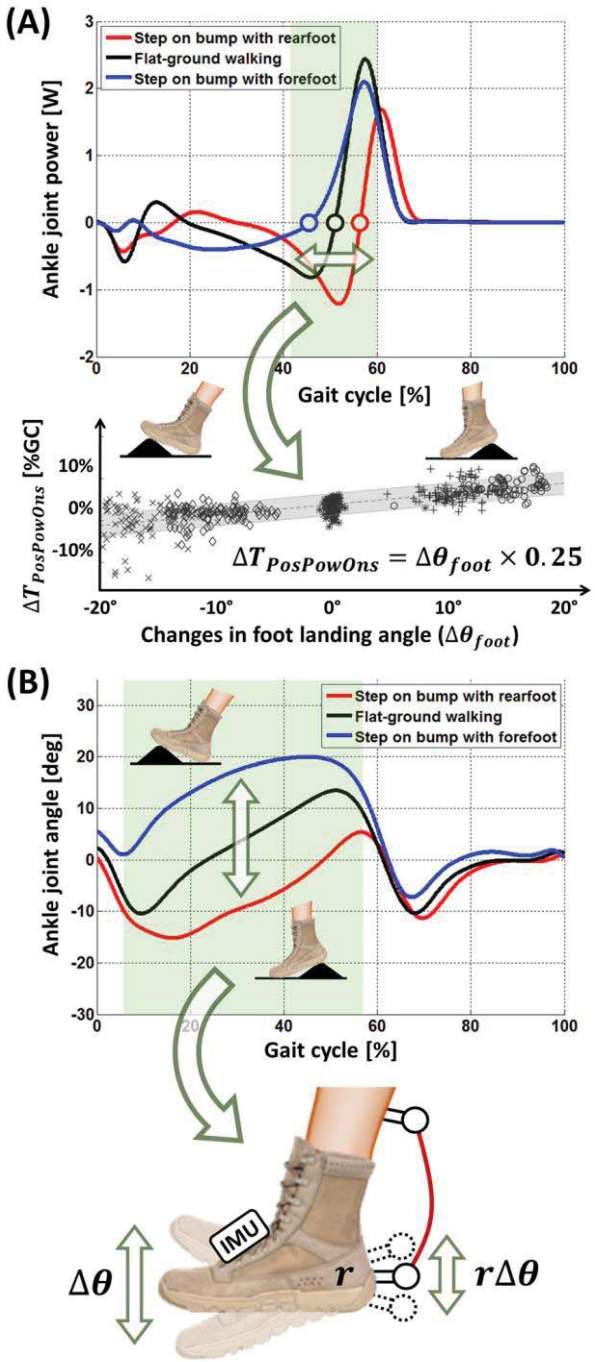

Figure 4 Biological insights for the control adaptation method for mild uneven terrain, gained from our previous study where the participants stepped on a small bump with either their forefoot or rearfoot while walking [21]. **(A)** The onset timing of positive power phase ($T_{PowPosOns}$) varies depending on changes in foot landing angle ($\Delta\theta_{Foot}$), and an empirical relation between the two was derived as follows: $\Delta T_{PosPowOns} = \Delta\theta_{Foot} \times (0.25)$. **(B)** The ankle joint angle during stance phase varies depending on foot contact conditions, and by using a simple 2-D kinematic model of ankle joint, the displacement of the boot attachment point can be modeled to be proportional to the changes in foot landing angle ($d_{BootAttach} = r \cdot \Delta\theta_{Foot}$).

V. Control Adaptation for Mild Uneven Terrain

As explained, the high-level controller was designed primarily based on lower-limb biomechanics during normal (flat-ground) walking. To improve step-to-step consistency of the assistance, and thus, to improve comfort and reliability of the exosuit during overground walking, an adaptive controller was developed by taking the kinetic and kinematic changes on irregular surfaces into consideration. First, (i) we further analyzed the data from our previous study [21] where the participants stepped on a small bump while walking, to gain biological insights on uneven terrain walking. Next, (ii) we translated these biological changes into control adaptation methods for exosuits. Finally, (iii) we conducted preliminary human walking experiments to evaluate the performance of the proposed method, presented in Section VI.

A. Biological Insights

Kinetic changes. When stepping on an irregular surface while walking, timing parameters defining biological ankle moment and power profiles vary depending on foot contact conditions, such as the onset/peak/offset of biological ankle moment and the onset of positive power phase [21]. In particular, as shown in Figure 4A, a strong linear correlation was found between the onset timing of the positive power phase and the foot landing angle; the positive power phase starts earlier when the foot landed more dorsiflexed and starts later when the foot landed more plantarflexed [21]. Based on experimental data over 9 subjects, an empirical relation between the changes in the onset of positive power phase ($\Delta \boldsymbol{T}_{\boldsymbol{PosPowOns}}$) and the changes in foot landing angle ($\Delta \boldsymbol{\theta}_{\boldsymbol{Foot}}$) compared to flat-ground walking was derived as follows:

$$\Delta \boldsymbol{T}_{\boldsymbol{PosPowOns}}\,[\%\mathrm{GC}] = \Delta \boldsymbol{\theta}_{\boldsymbol{Foot}}\,[\mathrm{deg}] \times (0.25) \quad \cdots (1)$$

Kinematic changes. When stepping on an uneven surface during walking, the ankle joint angle profile significantly varies depending on the foot landing angle, particularly during the stance phase, which can be explained as a direct result from the kinematic constraints imposed by the terrain [21]. With respect to the changes in ankle joint angle, the displacement of the cable attachment point at the back of the boot can be estimated by using a simple 2-D kinematic model of the ankle joint (Fig. 4B). Assuming a constant lever arm from the ankle joint center (100 mm), the displacement of the boot attachment point ($\boldsymbol{d}_{\boldsymbol{BootAttach}}$) would be proportional to the changes in foot landing angle ($\Delta \boldsymbol{\theta}_{\boldsymbol{Foot}}$):

$$\boldsymbol{d}_{\boldsymbol{BootAttach}}\,[\mathrm{mm}] = \Delta \boldsymbol{\theta}_{\boldsymbol{Foot}}\,[\mathrm{deg}] \times (\pi/180°) \times (100) \quad \cdots (2)$$

B. Control Implementation

Foot landing angle measurement. Given that both kinetic and kinematic changes at ankle can be predicted with respect to the foot landing angle, it would be important to measure this angle accurately on a step-by-step basis. In this study, the foot landing angle is estimated by averaging the sagittal-plane angle from the foot IMU from 10% to 30% of each gait cycle, only while the sagittal-plane gyro from the foot IMU is less than 50 dps (i.e. the foot is static on the ground). In an evaluation study where the IMU-estimated foot landing angle was compared with the ground truth measured by a motion capture system [22], RMS error on the estimation was 3.2 degrees which is sufficiently small for this application (Note

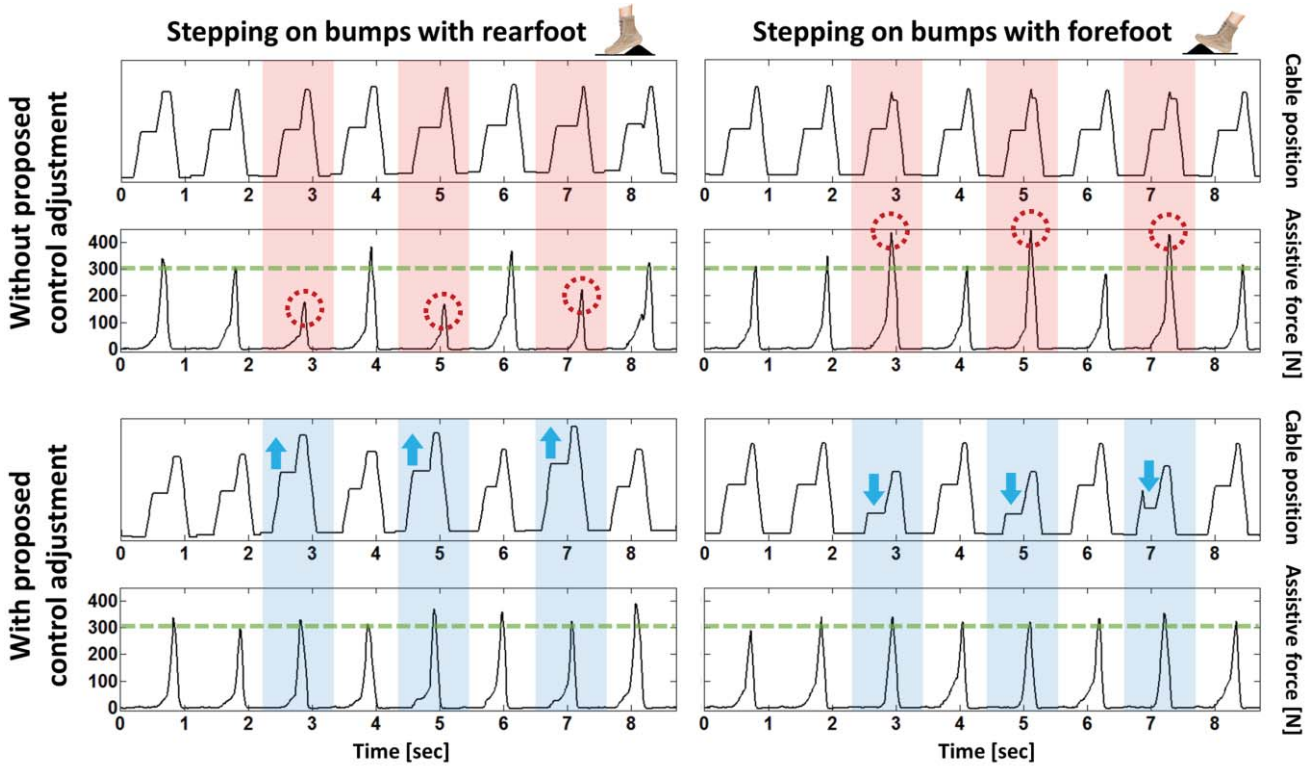

Figure 5 A representative data from the laboratory-based evaluation of the proposed control adaptation method for mild uneven terrain. Cable position and resultant force profiles on the multi-articular load path were compared when stepping on small bumps with rearfoot/forefoot and with/without the method. Shaded regions (red and blue) indicate the steps where the wearer contacted the bumps, and the green dotted lines indicate the target peak force (300 N). Without the method, the peak forces were much lower than the desired when stepping on the bumps with rearfoot (top left) and much higher when stepping with forefoot (top right). As shown in the bottom graphs, however, the proposed method adjusted the cable position in reaction to the step on the bump, substantially improving the step-to-step consistency of the peak force for both rearfoot (bottom left) and forefoot (bottom right) contact conditions.

that the foot landing angle usually deviates more than 10 degrees when stepping on irregular surfaces [21]).

Timing adaptation. Following the empirical relationship (1), the start timing of active force (***T1***), which corresponds to the onset of positive power phase, is adjusted based on the estimated foot landing angle ($\Delta\boldsymbol{\theta}_{Foot}$). When detected as a step on an uneven surface ($|\Delta\boldsymbol{\theta}_{Foot}|>10°$), the controller disregards the zero-crossing of ankle velocity measured by the IMUs for determining ***T1***; instead, the controller uses the averaged ***T1*** over the last three strides ($\boldsymbol{T1}_{Avg}$) as the baseline and adjusts the timing ($\boldsymbol{T1}^*$) following the heuristic equation (1):

$$\boldsymbol{T1}^*\,[\%GC] = \boldsymbol{T1}_{Avg}\,[\%GC] + \Delta\boldsymbol{\theta}_{Foot}\,[\text{deg}] \times (0.25) \quad \cdots (3)$$

Magnitude adaptation. As the force on the Bowden cable is determined by the relative position between the two cable attachment points, in order to maintain the same level of assistive force, the position controller of the cable has to offset the displacement of the attachment points. Thus, when detected as a step on an irregular surface ($|\Delta\boldsymbol{\theta}_{Foot}|>10°$), the cable position is adjusted ($\boldsymbol{P}^*$) based on the estimated foot landing angle ($\Delta\boldsymbol{\theta}_{Foot}$) following the equation (2), relative to the cable position in the previous stride ($\boldsymbol{P}_{Prev}$):

$$\boldsymbol{P}^*\,[\text{mm}] = \boldsymbol{P}_{Prev}\,[\text{mm}] + \Delta\boldsymbol{\theta}_{Foot}\,[\text{deg}] \times (100\cdot\pi/180) \quad \cdots (4)$$

VI. Preliminary Human Walking Experiments

A. Evaluation of the Control Adaptation for Uneven Terrain

Laboratory evaluation. Similar to [21], a single subject wearing the exosuit walked along a walkway involving three small bumps (height: 4.76 cm) on the ground at their preferred speed and stepped on the bumps with either their rearfoot or forefoot. The controller was commanded to generate peak forces of 300 N along the multi-articular load path, and the cable position and the resultant force profiles for versions of the controller with and without the proposed control adaptation were compared. As shown in Figure 5, the proposed method substantially improved the step-to-step consistency of the peak force in both foot contact conditions.

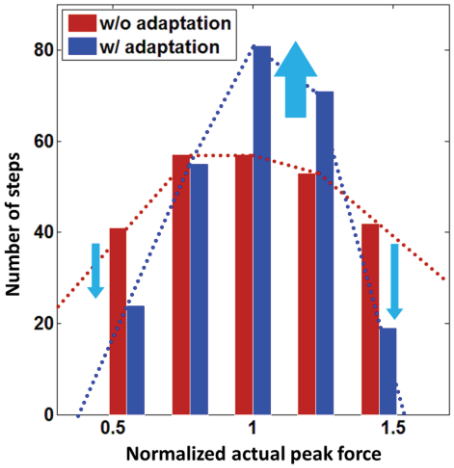

Figure 6 Peak force distributions while walking over a mild uneven terrain without (red) and with (blue) the proposed control adaptation method. The *x* axis indicates the measured peak force normalized by the target force (300 N), while the *y* axis indicates the number of steps out of 250 steps. As shown, the proposed control adaptation method made the peak force distribution much narrower, greatly reducing the number of steps where the peak force highly deviated from the target force.

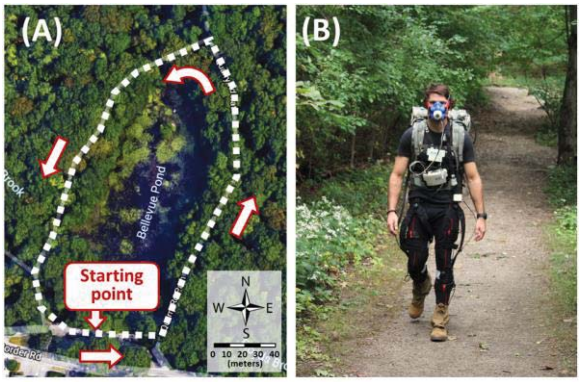

Figure 7 A case study on country-course walking. **(A)** A satellite view of the cross-country trail used in the study (42.4315°N, 71.1075°W; Google Maps; Google LLC, Mountain View, CA, USA). **(B)** A subject walking over the country course wearing the autonomous multi-joint soft exosuit and a portable indirect calorimetry (K4b2, COSMED, Rome, Italy) for metabolic evaluation.

Outdoors evaluation. A subject wearing the exosuit walked over a mild uneven terrain at their preferred speed, while the exosuit was commanded to generate peak forces of 300 N on the multi-articular load path. Measured peak forces during 250 steps were compared between with and without the proposed control adaptation method. As shown in Figure 6, the proposed control adaptation substantially improved the force consistency along the multi-articular load path, making the peak force distribution narrower. The number of steps where the peak force deviated more than 30% from the target force decreased from 100 to 57 steps out of 250 steps. This reduction in the number of inconsistent peak force can be explained by the fact that the proposed method was triggered in 55 steps out of 250 steps and adjusted the control profile. As a result, the RMS error for the peak force relative to the target force over 250 steps decreased from 90.0 N to 76.6 N.

B. Evaluation of the Autonomous Multi-Joint Soft Exosuit: Walking over a Country Course - A Case Study

As a proof-of-concept evaluation of the autonomous multi-joint soft exosuit, a two-subject case study was conducted where the participants walked over a country course carrying a load with and without wearing the device (Fig. 7). Two male adults (S1: 26 yrs, 83 kg, 177 cm; S2: 32 yrs, 77 kg, 170 cm) with sufficient experience of walking with exosuits participated in the study. A 500-m cross-country trail around Bellevue Pond in Middlesex Fells Reservation (Medford, MA, USA) was chosen as the site of experiment, which includes mild irregularities on the terrain (e.g. soil, mud, rocks, extruded tree roots, etc.). The trail consists of a mild uphill section at the beginning (approx. 200 m), a mild downhill section in the middle (approx. 100 m), and then a relatively flat section at the end (approx. 200 m). Each subject underwent two experimental conditions: *No-device* and *Active*. In each condition, the subjects continuously walked over the course for two laps (1 km in total) at their preferred speed carrying a 7-kg rucksack. During *Active* condition, the subjects wore the exosuit which applied peak assistive forces of 250 N for hip extension and 350 N for multi-articular assistance. The total device weighed 9.0 kg including a 48V-6.6Ahr battery (1.7 kg)

which is capable of approximately 5-km continuous walking operation. Considering that the exosuit controller was not optimized for slopes, the net metabolic cost during the last minute was compared, where the trail was relatively flat and the metabolic rate was at a steady-state.

As shown in Table I, for both participants, net metabolic rate substantially decreased in the *Active* condition compared to *No-device*, demonstrating the potential of the autonomous multi-joint soft exosuit to improve human energy economy during overground walking. While showing promising metabolic reduction, the 500-m lap time remained similar, indicating that the device didn't excessively affect the wearer's natural walking speed, even without the speed regulation usually given by a treadmill in lab-based studies.

TABLE I. RESULTS OF COUNTRY-COURSE WALKING TESTING

Subject / Condition		Net metabolic rate		500-m lap time
S1	***No-suit***	**3.69 W/kg**	**7.30% benefit**	**6 min 11 sec**
	Active	**3.42 W/kg**		**6 min 16 sec**
S2	***No-suit***	**5.42 W/kg**	**16.93% benefit**	**4 min 58 sec**
	Active	**4.51 W/kg**		**5 min 02 sec**

VII. CONCLUSION

In conclusion, we have presented the autonomous multi-joint soft exosuit for assistance with walking overground. All aspects of the system, i.e. apparel components, hardware elements, and controls, were improved over a previous autonomous system [13, 16], and the control adaptation for uneven terrain showed its capability to increase the force consistency of the exosuit while walking over an irregular surface. Although preliminary, the case study on country-course walking demonstrated the potential of the device to improve human walking economy overground. Of note, in a recent treadmill study using the same exosuit plus an on-line optimization algorithm that individualizes the control parameters [23], a 14.9% net metabolic reduction was found compared to a no-device condition.

Future work will include more thoroughly evaluating the performance and the efficacy of the exosuit while walking overground and developing methods to customize the control parameters to maximize the user's benefit [15, 23].

ACKNOWLEDGMENT

The authors would like to thank Taira Miyatake, Philippe Malcolm, Roman Heimgartner, Lauren Baker, Fausto A. Panizzolo, Andrew Long, Brice M. Iwangou, Dabin Choe, Adam Couture, and Sarah K. Sullivan for their contribution.

REFERENCES

[1] L. N. Awad, J. Bae, K. O'Donnell, S. M. M. De Rossi, K. Hendron, L. H. Sloot, P. Kudzia, S. Allen, K. G. Holt, T. D. Ellis, and C. J. Walsh, "A soft robotic exosuit improves walking in patients after stroke," *Sci Transl Med*, vol. 9, 2017.

[2] J. Bae, C. Siviy, M. Rouleau, N. Menard, K. O. Donnell, M. Athanassiu, D. Ryan, C. Bibeau, L. Sloot, P. Kudzia, T. Ellis, L. Awad, and C. J. Walsh, "A lightweight and efficient portable soft exosuit for paretic ankle assistance in walking after stroke," *in IEEE International Conference on Robotics and Automation (ICRA)*, 2018.

[3] P. Malcolm, W. Derave, S. Galle, and D. De Clercq, "A simple exoskeleton that assists plantarflexion can reduce the metabolic cost of human walking," *PLoS One*, vol. 8, 2013.

[4] S. H. Collins, M. B. Wiggin, and G. S. Sawicki, "Reducing the energy cost of human walking using an unpowered exoskeleton," *Nature*, vol. 522, 2015.

[5] L. M. Mooney and H. M. Herr, "Biomechanical walking mechanisms underlying the metabolic reduction caused by an autonomous exoskeleton," *J Neuroeng Rehabil*, vol. 13, 2016.

[6] L. M. Mooney, E. J. Rouse, and H. M. Herr, "Autonomous exoskeleton reduces metabolic cost of human walking during load carriage," *J Neuroeng Rehabil*, vol. 11, 2014.

[7] C. J. Walsh, K. Endo, and H. Herr, "A quasi-passive leg exoskeleton for load-carrying augmentation," *Int J Human Robot*, vol. 04, 2007.

[8] H. Herr, "Exoskeletons and orthoses: Classification, design challenges and future directions," *J Neuroeng Rehabil*, vol. 6, 2009.

[9] R. C. Browning, J. R. Modica, R. Kram, and A. Goswami, "The effects of adding mass to the legs on the energetics and biomechanics of walking," *Med Sci Sport Exerc*, vol. 39, 2007.

[10] J. Zhang, P. Fiers, K. A. Witte, R. W. Jackson, K. L. Poggensee, C. G. Atkeson, and S. H. Collins, "Human-in-the-loop optimization of exoskeleton assistance during walking," *Science*, vol. 23, 2017.

[11] J. Lee, K. Seo, B. Lim, J. Jang, K. Kim, and H. Choi, "Effects of assistance timing on metabolic cost, assistance power, and gait parameters for a hip-type exoskeleton," *in IEEE International Conference on Rehabilitation Robotics (ICORR)*, 2017.

[12] A. T. Asbeck, S. M. M. De Rossi, K. G. Holt, and C. J. Walsh, "A biologically inspired soft exosuit for walking assistance," *Int J Rob Res*, vol. 34, 2015.

[13] A. T. Asbeck, K. Schmidt, I. Galiana, D. Wagner, and C. J. Walsh, "Multi-joint soft exosuit for gait assistance," *in IEEE International Conference on Robotics and Automation (ICRA)*, 2015.

[14] B. T. Quinlivan, S. Lee, P. Malcolm, D. M. Rossi, M. Grimmer, C. Siviy, N. Karavas, D. Wagner, A. Asbeck, I. Galiana, and C. J. Walsh, "Assistance magnitude versus metabolic cost reductions for a tethered multiarticular soft exosuit," *Sci Robot*, vol. 2, 2017.

[15] Y. Ding, M. Kim, S. Kuindersma, and C. J. Walsh, "Human-in-the-loop optimization of hip assistance with a soft exosuit during walking," *Sci Robot*, vol. 3, 2018.

[16] F. A. Panizzolo, I. Galiana, A. T. Asbeck, C. Siviy, K. Schmidt, K. G. Holt, and C. J. Walsh, "Biologically-inspired multi-joint soft exosuit that can reduce the energy cost of loaded walking," *J Neuroeng Rehabil*, vol. 13, 2016.

[17] Y. Ding, I. Galiana, A. T. Asbeck, S. M. M. De Rossi, J. Bae, T. R. T. Santos, V. L. Araujo, S. Lee, K. G. Holt, and C. Walsh, "Biomechanical and physiological evaluation of multi-joint assistance with soft exosuits," *Trans Neural Syst Rehabil Eng*, vol. 25, 2017.

[18] G. Lee, J. Kim, F. A. Panizzolo, Y. M. Zhou, L. M. Baker, I. Galiana, P. Malcolm, and C. J. Walsh, "Reducing the metabolic cost of running with a tethered soft exosuit," *Sci Robot*, vol. 2, 2017.

[19] Y. Ding, I. Galiana, C. Siviy, F. A. Panizzolo, C. Walsh, "IMU-based iterative control for hip extension assistance with a soft exosuit," *in IEEE International Conference on Robotics and Automation (ICRA)*, 2016.

[20] S. Lee, S. Crea, P. Malcolm, I. Galiana, A. Asbeck, and C. Walsh, "Controlling negative and positive power at the ankle with a soft exosuit," *in IEEE International Conference on Robotics and Automation (ICRA)*, 2016.

[21] F. A. Panizzolo, S. Lee, T. Miyatake, D. M. Rossi, C. Siviy, J. Speeckaert, I. Galiana, and C. J. Walsh, "Lower limb biomechanical analysis during an unanticipated step on a bump reveals specific adaptations of walking on uneven terrains," *J Exp Biol*, vol. 220, 2017.

[22] T. Miyatake, S. Lee, I. Galiana, D. M. Rossi, C. Siviy, F. A. Panizzolo, and C. J. Walsh, "Biomechanical analysis and inertial sensing of ankle joint while stepping on an unanticipated bump," *in International Symposium on Wearable & Rehabilitation Robotics (WeRob)*, 2016.

[23] S. Lee, J. Kim, L. Baker, A. Long, N. Karavas, N. Menard, I. Galiana, C. J. Walsh, "Autonomous multi-joint soft exosuit with online optimization reduces energy cost of loaded walking," *J Neuroeng Rehabil*, submitted, 2018.